all at the molecular surface where they would be accessible to enzymes without any significant structural rearrangement, and second, at each of these sites (near favin residues 1, 110, and 182) the structures of favin and Con A differ only slightly and the differences are highly localized. Both molecules are apparently synthesized as precursors similar in three-dimensional structure to favin, but with a signal sequence at the NH_2-terminus and with residues 182 and 183 in favin joined by a peptide bond and local conformation similar to that between residues 69 and 70 in Con A.

In conclusion, the comparison of the superimposed molecules suggests that the differing biosynthetic patterns of the two molecules are of minimal significance for the function of the monomers. In all cases, peptide links that are missing in one or the other of the two proteins are located well away from the region of metal and saccharide binding and near to secondary structural features that would be expected to stabilize the structure near the "frayed ends" introduced by the various cleavages. The key features of the metal-binding region are nearly the same in the two structures, and the differences that are seen in the saccharide-binding region can be related to the differences in binding specificity of the two proteins. Further crystallographic refinement now in progress should provide a detailed picture of these interactions.

REFERENCES AND NOTES

1. H. Lis and N. Sharon, *Annu. Rev. Biochem.* **55**, 35 (1986).
2. M. E. Etzler, *Annu. Rev. Plant Physiol.* **36**, 209 (1985).
3. A. Foriers, C. Wuilmart, N. Sharon, A. D. Strosberg, *Biochem. Biophys. Res. Commun.* **75**, 980 (1977).
4. J. J. Hemperly and B. A. Cunningham, *Trends Biochem. Sci.* **8**, 100 (1983).
5. J. W. Becker, B. A. Cunningham, J. J. Hemperly, in *Chemical Taxonomy, Molecular Biology and Function of Plant Lectins*, I. J. Goldstein and M. E. Etzler, Eds. (Liss, New York, 1983), pp. 31–45.
6. B. A. Cunningham, J. J. Hemperly, T. P. Hopp, G. M. Edelman, *Proc. Natl. Acad. Sci. U.S.A.* **76**, 3218 (1979).
7. A. Foriers, E. Lebrun, R. Van Rapenbusch, R. deNeve, A. D. Strosberg, *J. Biol. Chem.* **256**, 5550 (1981).
8. J. J. Hemperly, K. E. Mostov, B. A. Cunningham, *ibid.* **257**, 7903 (1982).
9. D. J. Bowles *et al.*, *J. Cell Biol.* **102**, 1284 (1986).
10. J. W. Becker, G. N. Reeke, Jr., J. L. Wang, B. A. Cunningham, G. M. Edelman, *J. Biol. Chem.* **250**, 1513 (1975).
11. G. N. Reeke, Jr., J. W. Becker, G. M. Edelman, *ibid.*, p. 1525.
12. K. D. Hardman and C. F. Ainsworth, *Biochemistry* **11**, 4910 (1972).
13. E. J. Meehan, Jr., J. McDuffie, H. Einspahr, C. E. Bugg, F. L. Suddath, *J. Biol. Chem.* **257**, 13278 (1982).
14. R. R. Riskulov *et al.*, *FEBS Lett.* **165**, 97 (1984).
15. J. W. Becker, G. N. Reeke, Jr., G. M. Edelman, *Nature (London)* **259**, 406 (1976).
16. K. D. Hardman and C. F. Ainsworth, *Biochemistry* **15**, 1120 (1976).
17. J. L. Wang, J. W. Becker, G. N. Reeke, Jr., G. M. Edelman, *J. Mol. Biol.* **88**, 259 (1974).
18. H. Einspahr, E. H. Parks, K. Suguna, E. Subramanian, F. L. Suddath, *J. Biol. Chem.*, in press.
19. R. A. Crowther, in *The Molecular Replacement Method*, M. G. Rossmann, Ed. (Gordon and Breach, New York, 1972), pp. 173–185.
20. R. A. Crowther and D. M. Blow, *Acta Crystallogr.* **23**, 544 (1967).
21. W. A. Hendrickson and J. H. Konnert, in *Computing in Crystallography*, R. Diamond, S. Rameseshan, K. Venkatesan, Eds. (Indian Academy of Sciences, Bangalore, 1980), pp. 13.01–13.23.
22. G. A. Sim, *Acta Crystallogr.* **13**, 511 (1960).
23. A. N. Allen, N. N. Desai, A. Neuberger, *Biochem. J.* **155**, 127 (1976).
24. T. P. Hopp, J. J. Hemperly, B. A. Cunningham, *J. Biol. Chem.* **257**, 4473 (1982).
25. A. Jones, *J. Appl. Crystallogr.* **11**, 268 (1978).
26. G. N. Reeke, Jr., *ibid.* **17**, 125 (1984).
27. G. N. Reeke, Jr., J. W. Becker, G. M. Edelman, *Proc. Natl. Acad. Sci. U.S.A.* **75**, 2286 (1978).
28. R. D. Brown, C. F. Brewer, S. H. Koenig, *Biochemistry* **16**, 3883 (1977).

29. We thank F. L. Suddath and his colleagues for making available their coordinates for pea lectin in advance of publication. We also thank A. R. Fraser, J. J. Hemperly, and W. E. Gall for their contributions to earlier stages of this project, and especially G. M. Edelman and B. A. Cunningham for their advice and encouragement. Technical assistance was provided by S. Marglin. Atomic coordinates will be deposited with the Protein Data Bank upon completion of the crystallographic refinement now in progress. This work was supported by USPHS grant AI-11378, NSF grant PCM7709377, and development of computer programs by USPHS grant GM-22663.

16 July 1986; accepted 23 September 1986

Reversible Interconversion of Two Forms of a Valyl-tRNA Synthetase–Containing Protein Complex

SIMON BLACK

When an enzyme-containing complex from yeast was incubated in a buffered solution at room temperature, the valyl–transfer RNA synthetase activity and total protein oscillated synchronously between two physical states. This observation suggests a regulatory process that controls a number of enzymes as a group, an integrated function of a kind not heretofore recognized. The two forms of the complex were separated by ammonium sulfate precipitation of one of them in samples withdrawn from the incubated solution every 30 seconds. Glutathione and dithiothreitol in high concentrations (50 m*M*) enhance formation of the 50% saturated ammonium sulfate–soluble form. Oxidized glutathione, diphosphopyridine nucleotide, triphosphopyridine nucleotide, and a mercurial thiol binding agent in moderate concentrations (0.1 to 1.0 m*M*) shift the distribution toward the precipitable form. It is suggested that the two forms represent functional and nonfunctional complex-bound enzymes which are interconverted in response to oxidoreductive signals.

THE HYPOTHESIS THAT THE THIOL and disulfide groups on the surfaces of many enzyme molecules participate in the regulation of catalytic rates has a long history (*1*) and is well supported for certain photosynthetic systems (*2*). Evidence that these groups may participate in regulating the first step of protein biosynthesis, the aminoacylation of transfer RNA (tRNA), is provided by a valyl-tRNA synthetase-containing complex (*3, 4*). The synthetase requires a thiol for an activation process that is blocked by arsenite, which is a strong binder of pairs of adjacent thiol groups (*3*). It has now been found that when the complex is incubated in a buffered solution at room temperature, at a concentration about 100-fold greater than is used in enzyme activity tests, a rapid oscillatory change in state occurs that is affected by oxidoreductive and thiol-reactive agents. The change in state is evident from a change in the solubility of the complex in 50% saturated ammonium sulfate. These findings suggest a new function for the thiol group in a novel synchronous regulation of several enzymes associated in a complex.

The unstable complex used in the experiments was prepared from concentrated yeast cell sap (*3*), and would probably not survive the dilution accompanying more conventional procedures for isolating enzymes.

In the first experiment, the enzyme activities alternated between the supernatant and precipitate fractions (Fig. 1A), and total protein behaved similarly (Fig. 1B). Arsenite, which was present in this experiment, was assumed to be oxidoreductively neutral in the test environment. When arsenite was omitted, the oscillation was faster but deteriorated rapidly after 1 to 3 minutes. In 50 m*M* inorganic sulfide (Fig. 2), the most rapid oscillation was too fast to be adequately characterized with the present procedure, but well-defined cycles were evident between 3.5 and 8.5 minutes. In the presence of thiols (1.0 to 10 m*M*) or inorganic sulfide (5 to 50 m*M*), oscillatory interconversion continued for several hours, after which 80 to 90% of the enzyme activity and 60 to

Section on Pharmacology, Laboratory of Biochemical Pharmacology, National Institute of Diabetes and Digestive and Kidney Diseases, Bethesda, MD 20892.

70% of the protein remained in the supernatant form. Under these reducing conditions, the enzyme activity in both forms was completely stable for at least 16 hours.

In glutathione (GSH) of low concentration (Fig. 3), precipitable and supernatant forms of the enzyme varied within approximately equal ranges, as did the two forms of total protein, whereas with a high GSH concentration (Fig. 4) the supernatant forms of enzyme and total protein predominated. Dithiothreitol (50 m*M*) produced a result comparable to that with 50 m*M* GSH. In contrast, in 0.1 m*M* oxidized glutathione (GSSG) the majority of both enzyme activity and total protein in most fractions was in the precipitable state (Fig. 5). Enzyme activity and total protein distribution between soluble and precipitable forms were affected to different degrees in both 50 m*M* GSH (Fig. 4) and 0.1 m*M* GSSG (Fig. 5).

In the presence of NADP (Fig. 6), after 2 minutes of incubation, both enzyme activity and total protein remained predominantly in the precipitable form, and the interconversion process then seemed completely inhibited (*5*). A large variation within the precipitable enzyme fraction apparently signifies an interconversion between an active and an inactive state (*6*). NAD produced effects similar to those of NADP, including the large variation in the precipitable enzyme activity.

The thiol-binding agent *p*-chloromercuriphenylsulfonate (Fig. 7) maintained a major part of the enzyme activity and protein in the precipitable form during most of the cycles. The pattern was comparable to that found with GSSG (Fig. 5), which, through disulfide interchange, may also bind thiol groups.

In other experiments, 0.1 m*M* iodoacetate was found to stop the interconversion process almost instantaneously, whereas it completely inactivated the enzyme activity only after 1 to 2 hours. The effects of *N*-ethylmaleimide were similar, confirming the impression that unusually reactive thiol groups are exposed during oscillation. In the presence of these agents, total protein remained about equally divided between soluble and precipitable forms. Flavin mononucleotide, 0.1 m*M*, also stopped oscillation rapidly, inactivated the enzyme in the course of an hour, and left the protein equally divided between the two forms. The reduced pyridine nucleotides did not produce clearly defined oscillation patterns, and did not appear to act in the same way as NAD, NADP, or GSH. Oscillatory interconversion occurred when the reaction mixture was stirred or maintained under N_2.

Regulation of any biochemical process must involve an oscillation, because opposing influences cause alternate rises and falls in the concentration of a participating substance; such regulatory oscillation has been widely observed (*7*). The oscillatory cycles of 50% saturated ammonium sulfate–solu-

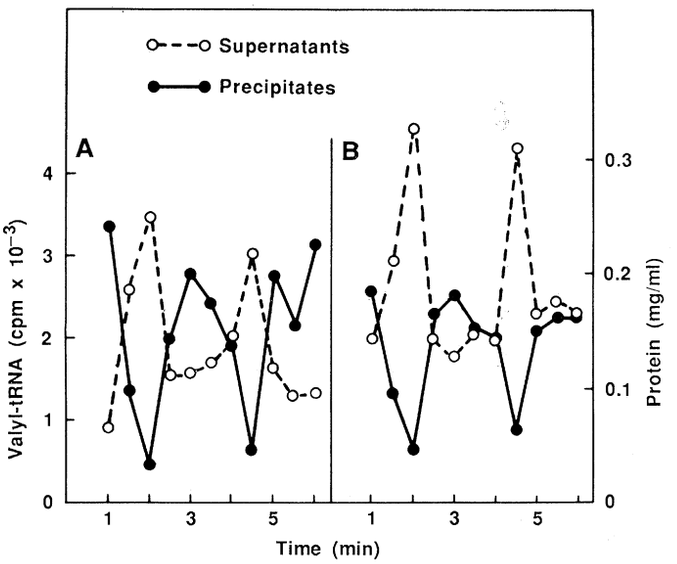

Fig. 1 (left). Distribution of 50% saturated ammonium sulfate–precipitable and supernatant forms of an enzyme activity (A) and total protein (B) after dilution of a complex enzyme preparation in tris buffer plus 5 m*M* arsenite. At time zero, 75 μl of the complex solution (*15*) (0.18 mg of protein) was diluted to a final volume of 0.6 ml, containing 0.2*M* tris chloride buffer, *p*H 8.0, and 5 m*M* sodium arsenite. The mixture was incubated in a water bath at 21°C in a 12 mm × 75 mm glass tube. Beginning 1 minute after adding the complex, 50-μl samples were withdrawn at 30-second intervals for rapid mixing with 50-μl portions of saturated ammonium sulfate held in 0.5-ml Eppendorf tubes in an ice bath. Mixing was achieved by pumping the contents of each tube in and out of a pipetter tip with a 200-μl capacity Pipetman pipetter set at 50 μl. Fifteen minutes after withdrawing the last sample, the precipitates were sedimented in the cold and the supernatants transferred to another set of 0.5-ml Eppendorf tubes in an ice bath. The precipitates were dissolved in 50 μl of 10 m*M* GSH brought to *p*H 8.0 with tris base. Five microliters of each supernatant and precipitate solution were then assayed for valyl-tRNA synthetase activity as described (*3*). Values for (A) represent 5 μl of the reaction mixture prior to ammonium sulfate addition. After assay all samples were frozen at −100°C for later protein determinations by the Bradford method (*16*). Bovine serum albumin was used as the protein standard. Values for (B) represent 1 ml of the reaction mixture prior to the addition of ammonium sulfate. Fig. 2 (top right). Distribution of precipitable and nonprecipitable enzyme activity (A) and protein (B) after dilution of a complex enzyme preparation in tris buffer plus

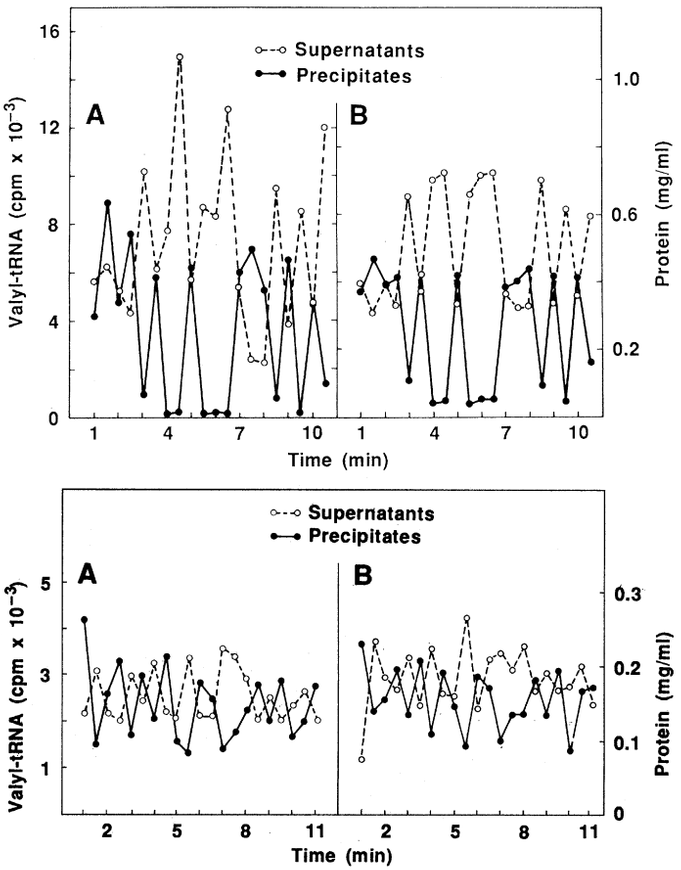

inorganic sulfide. The experiment was performed as described in the legend to Fig. 1 except that the reaction mixture contained 0.2*M* tris buffer, *p*H 8.0, plus 50 m*M* sulfide (obtained by mixing Na_2S and tris chloride, *p*H 7.0, in a 1:4 molar ratio); 1.08 mg of the complex protein in 0.3 ml of water was added last to bring the final volume to 1.2 ml. Fig. 3 (bottom right). Distribution of precipitable and nonprecipitable enzyme activity (A) and protein (B) after dilution of a complex enzyme preparation in tris buffer plus 0.2 m*M* GSH. The final reaction volume was 1.2 ml, containing 0.2*M* tris buffer, *p*H 8.0, and 0.2 m*M* GSH, after addition of 0.15 ml of the complex solution containing 0.36 mg of protein. The procedure is described in the legend to Fig. 1.

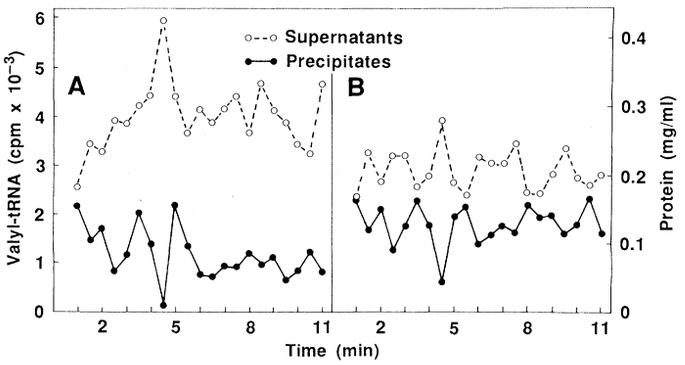

Fig. 4. Distribution of precipitable and nonprecipitable enzyme activity (A) and protein (B) after dilution of a complex enzyme preparation in tris buffer plus 50 m*M* GSH. The final reaction volume was 1.2 ml, containing 0.2*M* tris buffer, *p*H 8.0, and 50 m*M* GSH, after addition of 0.15 ml of the complex solution containing 0.36 mg of protein. The procedure is described in the legend to Fig. 1.

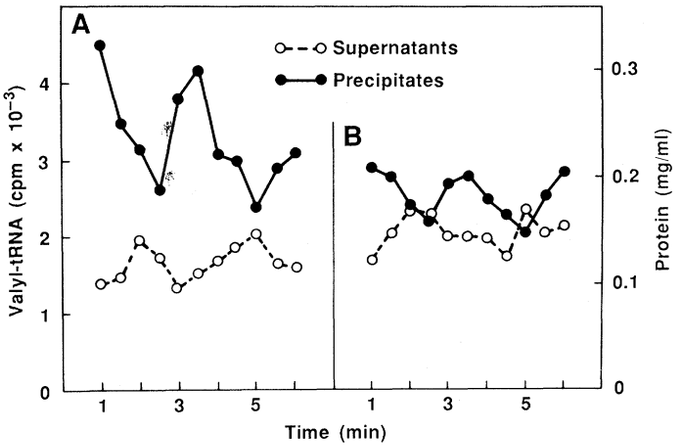

Fig. 5. Distribution of precipitable and nonprecipitable enzyme activity (A) and protein (B) after dilution of a complex enzyme preparation in tris buffer plus 0.1 m*M* GSSG. The final reaction volume was 0.6 ml, containing 0.2*M* tris buffer, *p*H 8.0, and 0.1 m*M* GSSG, after addition of 0.075 ml of the complex solution containing 0.18 mg of protein. The procedure is described in the legend to Fig. 1.

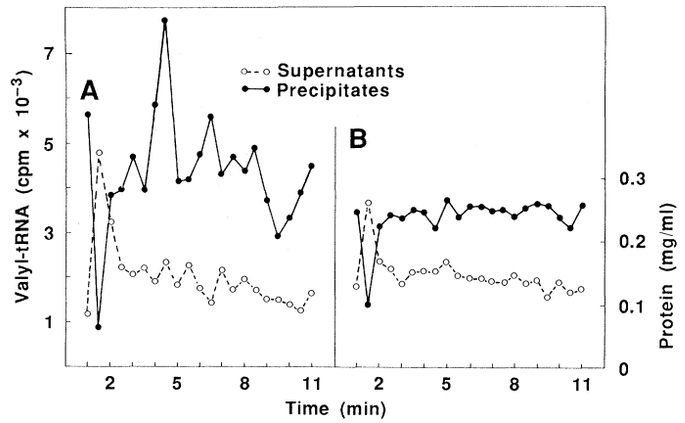

Fig. 6. Distribution of precipitable and nonprecipitable enzyme activity (A) and protein (B) after dilution of a complex enzyme preparation in tris buffer plus 1 m*M* NADP. The final reaction volume was 1.2 ml, containing 0.2*M* tris buffer, *p*H 8.0, and 1 m*M* NADP, after addition of 0.15 ml of the complex solution containing 0.36 mg of protein. The procedure is described in the legend to Fig. 1.

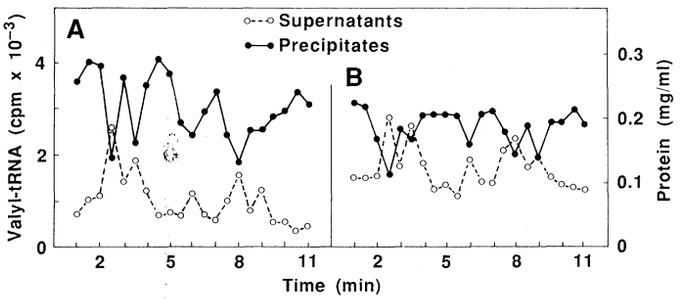

Fig. 7. Distribution of precipitable and nonprecipitable enzyme activity (A) and protein (B) after dilution of a complex enzyme preparation in tris buffer plus 1 m*M* *p*-chloromercuriphenylsulfonate. The final reaction volume was 1.2 ml, containing 0.2*M* tris buffer, *p*H 8.0, and 1 m*M* *p*-chloromercuriphenylsulfonate, after addition of 0.15 ml of the complex solution containing 0.36 mg of protein. The procedure is described in the legend to Fig. 1.

ble and –insoluble protein fractions recorded in Figs. 1 and 2 have adequate range and rapidity to qualify for a regulatory function, and the influence of oxidoreductive and thiol-reactive agents on the distribution between forms (Figs. 4 to 7) implicates the participation of the protein thiol group in such a function. The synchrony of valyl-tRNA synthetase oscillation with that of a group of 15 or so other proteins implies functional linkage and reinforces the conclusion (*3*) that these proteins are physically associated as a complex.

The components of the nonprecipitable fractions may be more readily available for function than the precipitable components, but in the case of the complex-bound valyl-tRNA synthetase an additional reduction step is needed to produce an active enzyme. Even fractions that have been incubated with 5 m*M* dithiothreitol or inorganic sulfide during interconversion experiments require a thiol for full activity in the assay system. Further evidence that the thiol-dependent activating mechanism for this enzyme (*3*) is not an obligatory part of the interconversion mechanism is found in the relative insensitivity of the oscillation to arsenite (Fig. 1). Whereas arsenite completely blocks the reductive activation, it only slows the oscillation, as evident from a comparison of the first few cycles of Figs. 1 and 2. The slowing may indicate that the reductive activation mechanism is in some way coupled to the oscillatory function but not essential to it.

A potential regulator is GSSG, which, in low concentrations, has a pronounced effect on the cycling rate and on the distribution of enzyme and protein between precipitable and supernatant forms (compare Fig. 5 with Figs. 3 and 4). GSSG has been previously proposed as a regulator of protein biosynthesis (*8, 9*). Other candidate regulators are NADP (Fig. 6) and NAD, which strongly inhibit the interconversion of ammonium sulfate–separable forms and favor maintenance of the precipitable relative to the soluble fraction.

Whether this easily dissociable, labile complex is closely related to the more stable aminoacyl-tRNA synthetase complexes of animal tissues is problematic (*10–13*), but an evolutionary relationship is conceivable [see (*14*)].

REFERENCES AND NOTES

1. D. M. Ziegler, *Annu. Rev. Biochem.* **54**, 305 (1985).
2. B. B. Buchanan, in *Functions of Glutathione*, A. Larsson, S. Orrenius, A. Holmgren, B. Mannervik, Eds. (Raven, New York, 1983), pp. 331–342.
3. S. Black, *J. Biol. Chem.* **258**, 2112 (1983).
4. ———, *ibid.* **260**, 433 (1985).
5. Abbreviations used are NAD (diphosphopyridine nucleotide) and NADP (triphosphopyridine nucleotide).
6. An inactive, that is, undetectable, intermediate in the enzyme interconversion in the slowest cycles of Fig. 2 is suggested by a lag in the rise of supernatant activity after the precipitate values have reached zero, and by some imperfections in the reciprocal relation in other experiments.
7. B. Chance, E. K. Pye, A. K. Ghosh, B. Hess, Eds.,

Biological and Biochemical Oscillators (Academic Press, New York, 1973).
8. N. S. Kosower, G. A. Vanderhoff, B. Benerofe, T. Hunt, E. M. Kosower, *Biochem. Biophys. Res. Commun.* **45**, 816 (1971).
9. A. Meister, in *Metabolic Pathways*, D. M. Greenberg, Ed. (Academic Press, New York, ed. 3, 1975), vol. 7, pp. 101–188.
10. A. K. Bandyopadhyay and M. P. Deutscher, *J. Mol. Biol.* **60**, 113 (1971).
11. M. P. Deutscher, *J. Cell Biol.* **99**, 373 (1984).
12. C. V. Dang *et al.*, *FEBS Lett.* **142**, 1 (1982).
13. M. Mirande, B. Cirakoğlu, J.-P. Waller, *J. Biol. Chem.* **257**, 11056 (1982).
14. B. Cirakoğlu and J.-P. Waller, *Eur. J. Biochem.* **149**, 353 (1985).
15. The valyl-tRNA synthetase–containing complex was prepared essentially as described (*3*) except that the fraction precipitated between 25% and 50% saturated ammonium sulfate was used instead of the 39 to 50% fraction. A solution of three-times precipitated material in 0.5*M* ammonium sulfate–0.05*M* tris buffer, *p*H 8.0, was freed of opalescence by centrifuging for 1 hour in the cold at 30,000 rpm. A final precipitate from cold 50% saturated ammonium sulfate was divided as a suspension for centrifugation in 0.5-ml Eppendorf tubes to obtain 0.36 mg of protein per tube for storage at −100°C. Immediately before use a precipitate was dissolved in water to the protein concentration indicated in the legend to each figure. On electrophoresis in a 10% polyacrylamide gel with SDS, the complex preparation used in the experiments described here, yields 15 bands that stain in widely varying degree with Coomassie Blue and have molecular weights of 20,000 to 100,000. The most heavily stained bands are a pair near the 29,000 molecular weight marker. Of 14 other aminoacyl-tRNA synthetases tested, the activities for lysine, arginine, and threonine were 40%, 7%, and 3.6%, respectively, of that for valine, and all others were less than 1%. The preparation represents about 3% of the extractable protein of baker's yeast cake (Anheuser-Busch). The results shown in the figures are typical of those obtained in several repetitions of each experiment under closely similar conditions, involving two different preparations of the enzyme-containing complex. The oscillations are readily reproducible. They always occur under a given set of conditions if not inhibited in some way, as in the experiment of Fig. 6.
16. M. Bradford, *Anal. Biochem.* **72**, 248 (1976).
17. I thank D. Black for technical assistance.

7 August 1986; accepted 10 October 1986

Long-Term Downward Trend in Total Solar Irradiance

R. C. WILLSON, H. S. HUDSON, C. FROHLICH, R. W. BRUSA*

The first 5 years (from 1980 to 1985) of total solar irradiance observations by the first Active Cavity Radiometer Irradiance Monitor (ACRIM I) experiment on board the Solar Maximum Mission spacecraft show a clearly defined downward trend of −0.019% per year. The existence of this trend has been confirmed by the internal self-calibrations of ACRIM I, by independent measurements from sounding rockets and balloons, and by observations from the Nimbus-7 spacecraft. The trend appears to be due to unpredicted variations of solar luminosity on time scales of years, and it may be related to solar cycle magnetic activity.

THE TOTAL SOLAR IRRADIANCE OF the earth is the primary determining factor of climate. Sustained variations from the present average value could alter the terrestrial environment. Systematic changes in irradiance of as little as 0.5% per century can cause the complete range of climate variations that have occurred in the past, ranging from ice ages to global tropical conditions (*1*). Knowledge of solar trends is important for understanding the interaction between solar variability and terrestrial climate-forcing phenomena, such as natural or man-made changes in atmospheric composition.

Our present knowledge of the interior of the sun does not allow for accurate predictions of solar luminosity (which we assume to be proportional to the total solar irradiance measured at the earth over long time scales). We must therefore depend on high-precision observations of the solar irradiance over time scales of climatological significance to understand the sun's role in climate variability. The secondary objective of compiling an irradiance database is to improve knowledge of solar physical processes that could provide a predictive capability for solar irradiance variations.

The modern high-precision database on solar total irradiance was started in 1980. It used data from the first Active Cavity Radiometer Irradiance Monitor (ACRIM I) experiment on the National Aeronautics and Space Administration's (NASA) Solar Maximum Mission (SMM) spacecraft (*2*). These observations have a precision of a few parts per million per day, based on the statistics of about 400 time-averaged samples per day. The ACRIM I observations now extend over a period of about one-half of a solar sunspot cycle.

Some observed irradiance variations have been related to known solar phenomena. The largest deviations from the mean are temporary decreases in irradiance of up to 0.25% on time scales of days, which have been shown to have a clear correlation with sunspots (*2–4*). A facular signal is also present at the level of +0.1% or less on time scales of weeks to months (*4–6*), but it is not as well understood, partly because of its smaller amplitude and the poor record of facular presence and properties.

On a shorter time scale the ACRIM I data reveal that solar global oscillations with a period near 5 minutes produce detectable irradiance variations with amplitudes for low degree modes of up to a few parts per million in the total irradiance (*7, 8*). These oscillations appear as resonance peaks in the power spectrum, superposed on a continuum of variation assumed to be due to the granulation and other atmospheric structures of the sun in the absence of significant solar magnetic activity (*9*).

This report focuses on the longest ACRIM I time scale, extending from the launch in February 1980 to the end of 1984, approximately one-half of an 11-year sunspot cycle. We provide a characterization of the slowest variations observed from the ACRIM I data. The longest time scales present the most difficulty for sustaining instrument calibration, but they are at the same time potentially the most important from the point of view of geophysical or astrophysical consequences.

The ACRIM I database used is essentially the same one published by the National Oceanic and Atmospheric Administration (NOAA) in *Solar-Geophysical Data* and described by Willson (*2, 4, 5*). The database derived from the observations consists of

Table 1. Results of sounding rocket and balloon solar irradiance reference experiments shown as the difference between their ratios, and SMM/ACRIM I observations taken on or near the same day.

Mission day*	ACRIM I (W/m^2)	ACR rocket (ppm)	PMOD balloon and rocket (ppm)
141	1368.5	−365	
1275	1367.4		−293
1437†	1367.5	−73	−585
1806	1367.0	73	−146
Average		−122	−341
SD		223	223

*SMM day count beginning with 1 January 1980. †The ACRIM I result from day 1434 was used since it was the nearest available.

R. C. Willson, Jet Propulsion Laboratory, California Institute of Technology, Pasadena, CA 91109.
H. S. Hudson, Center for Astrophysics and Space Science, University of California at San Diego, La Jolla, CA 92093.
C. Frohlich and R. W. Brusa, World Radiation Center, Physikalisch-Meteorologisches Observatorium, Davos, CH-7260 Davos Dorf, Switzerland.

*Present address: Space Science Department, European Space Technology Centre, European Space Agency, Noordwijk, the Netherlands.